

THE ANALYSIS OF CYLINDRICAL SHELL ROOFS WITH POST TENSIONED EDGE BEAMS

RAPHAEL FONER RISH†

University of Tasmania, Box 252C G.P.O., Hobart, 7001, Tasmania, Australia

(Received 13 August 1973; revised 25 February 1974)

Abstract—A new characteristic equation for cylindrical shell roofs is developed, together with a method for obtaining the solution and its derivatives. Post tension is introduced into the edge beam by shearing forces varying linearly from a maximum at the transverse to zero at the quarter points. The Fourier series for this converges rapidly. An end correction is then made to restore the post tension to the end of the edge beam and obtain compatibility of strain with the shell edge. The method is compared with experimental results on a model shell and with the results of a finite element program.

NOTATION

u, v, w	Longitudinal, circumferential, radial displacements, ft
N_x, N_ϕ, S	longitudinal, circumferential, shearing forces, lb/ft
$\epsilon_x, \epsilon_\phi, \gamma_{x\phi}$	longitudinal, circumferential, shearing strains
$M_x, M_\phi, M_{x\phi}$	longitudinal, circumferential, twisting moments, lb
Q_x, Q_ϕ	normal shearing forces, lb/ft
V_ϕ	normal force at edge, lb/ft
x (ft), ϕ (rad)	longitudinal, radial coordinates,
a	angular rotation of shell, rad
R, L, h	radius, length, thickness of shell, ft
ϕ_K	half angle of shell, rad
E	Young's modulus, lb/ft ²
ν	Poisson's ratio
D	flexural rigidity of shell, lb ft
N	integer in Fourier series term
m	$N\pi R/L$
k, θ	parametric constants
$4K^4$	$12(1 - \nu^2)R^2/h^2$
p	a root of the characteristic equation
A (ft ²), J (ft ⁴)	area, moment of inertia of edge beam
P	post tension load in edge beam, lb
T	torque on edge beam, lb ft
t	force at springing due to shear, lb.

INTRODUCTION

Cylindrical shell roofs are used to provide an economical way of covering large areas without intermediate supports. The first cylindrical shell of the type shown in Fig. 1 was built in Germany in 1925. The number of these structures now in existence is very large.

The shell is constructed in reinforced concrete about three inches thick. This gives sufficient cover to protect the reinforcement. The main loading is the self weight of the shell and a layer of snow. Wind blowing across the shell produces a uniform uplift and can normally be neglected.

† Senior Lecturer, Department of Civil Engineering.

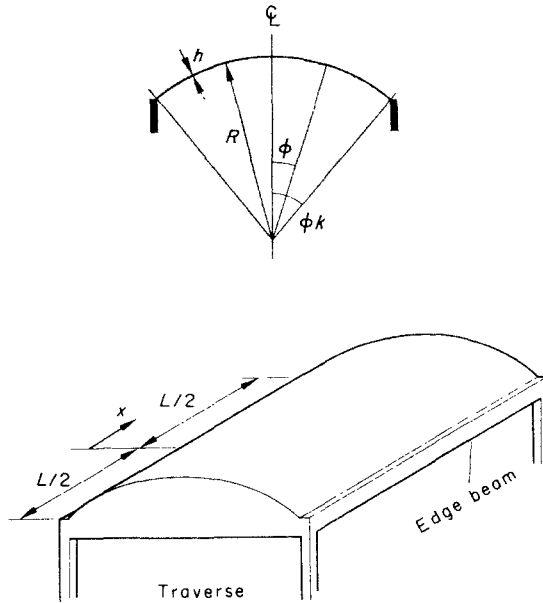


Fig. 1. Cylindrical shell roof.

Edge beams are provided to stiffen the edges of the longer shells and these edge beams are frequently post-tensioned to reduce the amount of reinforcement required in the shell.

The traverses are thin and the assumption that they do not present any resistance to horizontal movement enables a linear differential equation to be developed for the deflection of the shell. Flügge[1] has developed this differential equation with the minimum of approximation. As he points out, the mathematical manipulation of such a system is far from simple. The roots of the auxiliary equation arising from Flügge's equation are difficult to extract accurately and the force-deformation relations are very complicated.

This paper shows how Flügge's equation can be simplified without serious loss of accuracy using Ferrari's method for the solution of a quartic. The simplified equation has explicit roots which can be readily employed in the design of shell roofs.

The gravity loading of a cylindrical shell roof can then be handled on a small digital computer by using a sufficient number of terms of the Fourier series for the loading.

Attempts have been made to determine the stresses due to post-tension in a similar manner[2]. However in this case the errors increase with the number of terms employed. The difficulty is due to the assumption that the traverses cannot transmit any of the post-tension directly to the shell. Compatibility of strain between the edge beam and the shell becomes impossible to obtain close to the traverses. When the assumption is abandoned it becomes possible to handle the post tension in an economical manner.

THEORETICAL ANALYSIS

The characteristic equation

In a cylindrical shell the displacements vary with both x and ϕ . It will be assumed that the shell does not move radially at the traverses. It will also be taken initially that the traverses offer no resistance to horizontal displacement. The differential equation of the shell can then

be handled by taking the radial displacement as

$$w = Ae^{p\phi} \cos mx/R$$

where

$$m = N\pi R/L.$$

All forces and displacements in the shell then appear in terms of a Fourier series in x .

The auxiliary to Flügge's equation becomes

$$(p^2 - m^2)^4 + 4m^4K^4 + 2p^6 + Fp^4 + Gp^2 - 2vm^2 = 0 \tag{1}$$

where

$$\begin{aligned} 4K^4 &= 12(1 - \nu^2)R^2/h^2 \\ F &= 1 - 2(4 - \nu)m^2 \\ G &= 6m^4 - 2(2 - \nu)m^2. \end{aligned}$$

The auxiliary is a quartic equation in p^2 and the coefficients can be tabulated as follows:

p^8	p^6	p^4	p^2	1
1	$\frac{-4m^2}{2}$	$\frac{+6m^4}{+F}$	$\frac{-4m^6}{+G}$	$\frac{m^8}{+4m^4K^4}$ $\frac{-2m^6\nu}{-2m^6\nu}$
1	$2a$	b	$2c$	d

What happens next can best be shown by putting in numbers for a typical case. Using the dimensions of Gibson's long shell[3], $R = 30$ ft, $h = 0.25$ ft, $L = 120$ ft and $\nu = 0.15$, and taking the first term of the Fourier series $N = 1$, $m = \pi/4$ and $4K^4 = 168912$.

The table then becomes

p^8	p^6	p^4	p^2	1
1	-2.4674 $+2$	$+2.2830$ -3.7497	-0.9388 $+0.0006$	$+0.1448$ $+64271.185$ -0.0704
1	-0.4674	-1.4667	-0.9382	$+64271.259$

To solve the quartic

$$p^8 + 2ap^6 + bp^4 + 2cp^2 + d = 0$$

it will be assumed possible to express it as the difference of two squares

$$(p^4 + qp^2 + r)^2 - (sp^2 + t)^2 = 0 \tag{2}$$

or

$$p^8 + 2qp^6 + (q^2 + 2r + s^2)p^4 + 2(qr - st)p^2 + (r^2 - t^2) = 0.$$

On comparing coefficients

$$\begin{aligned} q &= a; & q^2 - 2r - s^2 &= b; \\ qr - st &= c; & r^2 - t^2 &= d. \end{aligned} \tag{3}$$

Eliminating s and t and substituting for q we obtain the cubic equation

$$r^3 - \frac{b}{2}r^2 + (ac - d)r + \frac{1}{2}[d(b - a^2) - c^2] = 0. \quad (4)$$

Putting in the numbers for our typical case the cubic becomes

$$r^3 + 0.7335r^2 - 64271.1497r - 4888.2214 = 0 \quad (5)$$

d is much larger than the other numbers in equation (4) and assuming that r has a small real value it is evident from inspection that r will be very nearly equal to $\frac{1}{2}(b - a)^2$ or -0.760668 . Evaluating (5) on a desk computer for trial values of r shows that the correct value of r is -0.760671 .

Now (2) can be expressed as:

$$(p^4 + qp^2 + r^2) + (sp^2 + t) = 0$$

and

$$(p^4 + qp^2 + r^2) - (sp^2 + t) = 0$$

or

$$p^4 + (q + s)p^2 + (r^2 + t) = 0$$

and

$$p^4 + (q - s)p^2 + (r^2 - t) = 0. \quad (6)$$

Transposing (3) it is found that $t = \sqrt{(r^2 - d)} = 2m^2K^2i$ as r^2 is negligible compared with d which is very nearly equal to $4m^4K^4$. $s = (qr - c)/t$ which is very small compared with q , and r^2 is very small compared with t .

The two quadratic equations in p^2 (6) then reduce to:

$$\begin{aligned} p^4 + ap^2 + t &= 0 \\ p^4 + ap^2 - t &= 0 \end{aligned}$$

hence

$$\begin{aligned} p^2 &= -\frac{a}{2} \pm \sqrt{\left(\frac{a^2}{4} \pm t\right)} \\ &= -\frac{a}{2} \pm \sqrt{\left(\frac{a^2}{4} \pm 2m^2K^2i\right)}. \end{aligned}$$

The imaginary part under the square root is much larger than the real so that

$$p^2 = -\frac{a}{2} \pm mK(\sqrt{2}i) = -\frac{1}{2} + m^2 + mK(\pm 1 \pm i). \quad (7)$$

This can be compared with the roots for Schorer's equation:

$$p^2 = mK(\pm 1 \pm i)$$

and with those of the widely used D.K.J. equation:

$$p^2 = m^2 + mK(\pm 1 \pm i). \tag{4}$$

It will be seen that for long shells, i.e. where $m^2 < 1/2$ the roots of Schorer's equation are more accurate than those of the D.K.J. equation.

If the factors in Table 1 that do not contribute towards (7) are eliminated we are left with the auxiliary equation:

$$p^8 - 4m^2p^6 + 2p^6 + 4m^4K^4 = 0$$

which corresponds to the dimensional characteristic equation

$$\frac{\partial^8 w}{\partial \phi^8} + 4R^2 \frac{\partial^8 w}{\partial \phi^6 \partial x^2} + 2 \frac{\partial^6 w}{\partial \phi^6} + 4K^4 R^4 \frac{\partial^4 w}{\partial x^4} = 0. \tag{8}$$

Before (8) can be used in design it is necessary to find the force-deformation relations corresponding to it. This was done by working back through Flügge's calculations and leaving out any terms that did not lead to the desired characteristic equation.

It appeared that M_x could be neglected as in Schorer's equation but not the twisting moment. That ϵ_ϕ could be considered small compared with w/R and $\partial v/R \partial \phi$ but that $\gamma_{x\phi}$ could not be neglected when compared with $\partial u/R \partial \phi$ and $\partial v/\partial x$. Other approximations leading to the desired result were the ignoring of vN_ϕ compared with N_x in the calculation of ϵ_x , the taking of $M_{x\phi}$ as $\frac{D(1-\nu)}{R} \frac{\partial^2 w}{\partial \phi \partial x}$ and M_ϕ as $-DX_\phi$. In general the method leads to the inclusion of first and second order terms and the neglect of higher order terms.

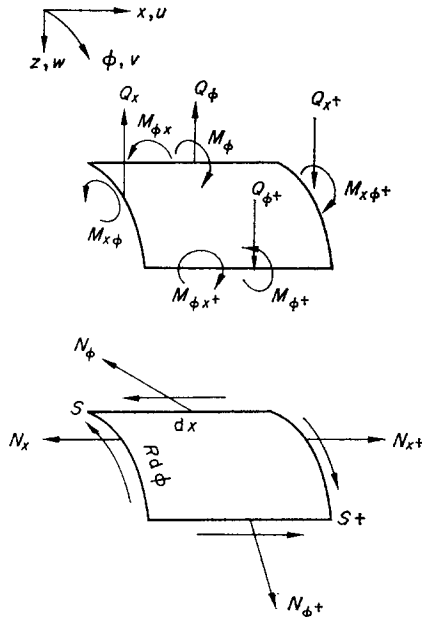


Fig. 2. Statics of element.

From the statics of the element in Fig. 2

$$\begin{aligned}
 Q_\phi &= \frac{\partial M_\phi}{R \partial \phi} - \frac{\partial M_{x\phi}}{\partial x} \\
 Q_x &= -\frac{\partial M_{x\phi}}{R \partial \phi} \\
 N_\phi &= -\frac{\partial Q_\phi}{\partial \phi} - \frac{R \partial Q_x}{\partial x} \\
 &= -\frac{\partial^2 M_\phi}{R \partial \phi^2} + 2 \frac{\partial^2 M_{x\phi}}{\partial \phi \partial x} \\
 \frac{\partial S}{\partial x} &= -\frac{\partial N_\phi}{R \partial \phi} + \frac{Q_\phi}{R} \\
 &= \frac{\partial^3 M_\phi}{R^2 \partial \phi^3} - \frac{2 \partial^3 M_{x\phi}}{R \partial \phi^2 \partial x} + \frac{\partial M_\phi}{R^2 \partial \phi} \\
 \frac{\partial N_x}{\partial x} &= -\frac{1}{R} \frac{\partial S}{\partial \phi} \\
 \frac{\partial^2 N_x}{\partial \phi^2} &= -\frac{1}{R} \frac{\partial}{\partial \phi} \left(\frac{\partial S}{\partial x} \right) \\
 &= -\frac{1}{R^3} \frac{\partial^4 M_\phi}{\partial \phi^4} + \frac{2}{R^2} \frac{\partial^4 M_{x\phi}}{\partial \phi^3 \partial x} - \frac{1}{R^3} \frac{\partial^2 M_\phi}{\partial x}.
 \end{aligned}$$

The force-deformation relations are:

$$\begin{aligned}
 M_\phi &= -\frac{D}{R^2} \left(\frac{\partial^2 w}{\partial \phi^2} + w \right) \\
 M_{x\phi} &= \frac{D(1-\nu)}{R} \frac{\partial^2 w}{\partial \phi \partial x} \\
 \epsilon_x &= \frac{\partial u}{\partial x} = \frac{N_x}{Eh} \\
 \epsilon_\phi &= \frac{1}{R} \left(\frac{\partial v}{\partial \phi} - w \right)
 \end{aligned}$$

this is considered small compared with the separate components on the R.H. side which are due mainly to bending

$$\begin{aligned}
 \therefore w &= \frac{\partial v}{\partial \phi} \\
 \gamma_{x\phi} &= \frac{\partial u}{R \partial \phi} + \frac{\partial v}{\partial x} = \frac{S}{Gh} = \frac{2(1+\nu)}{Eh} S \\
 \frac{\partial^4 w}{\partial x^4} &= \frac{\partial^5 v}{\partial \phi \partial x^4} = 2 \frac{(1+\nu)}{Eh} \frac{\partial^4 S}{\partial \phi \partial x^4} - \frac{\partial^5 u}{R \partial \phi^2 \partial x^3}
 \end{aligned}$$

$$\begin{aligned}
 -\frac{1}{R} \frac{\partial^5 u}{\partial \phi^2 \partial x^3} &= -\frac{1}{EhR} \frac{\partial^4 N_x}{\partial \phi^2 \partial x^2} \\
 &= -\frac{1}{EhR} \left\{ -\frac{\partial^6 M_\phi}{R^3 \partial \phi^6} + \frac{2 \partial^6 M_{x\phi}}{R^2 \partial \phi^5 \partial x} - \frac{\partial^4 M_\phi}{R^3 \partial \phi^4} \right\} \\
 &= -\frac{D}{EhR} \left\{ \frac{1}{R^5} \left(\frac{\partial^8 w}{\partial \phi^8} + 2 \frac{\partial^6 w}{\partial \phi^6} \right) + \frac{2(1-\nu)}{R^3} \frac{\partial^8 w}{\partial \phi^6 \partial x^2} \right\} \\
 \therefore \frac{\partial^8 w}{\partial \phi^8} + 2 \frac{\partial^6 w}{\partial \phi^6} + 4R^2 \frac{\partial^8 w}{\partial \phi^6 \partial x^2} + \frac{12(1-\nu^2)R^6}{h^2} \frac{\partial^4 w}{\partial x^4} &= 0.
 \end{aligned}$$

This is the same equation as (8).

The radial deflection in the shell will now be taken in the form

$$w = W \cos mx/R = W \cos N\pi x/L$$

where W is a function only of ϕ .

The deformations and forces at the centre of the shell where $x = 0$ can be expressed as derivatives of W with respect to ϕ . The values elsewhere can be obtained by multiplying by $\cos mx/R$

$$\begin{aligned}
 v &= \int W \, d\phi \\
 a &= \frac{1}{R} \left(\frac{dW}{d\phi} + v \right) \\
 M_\phi &= -\frac{D}{R^2} \left(\frac{d^2 W}{d\phi^2} + W \right) \\
 V_\phi &= Q_\phi - \frac{dM_{x\phi}}{dx} = -\frac{D}{R^3} \left\{ \frac{d^3 W}{d\phi^3} + [1 - 2(1-\nu)m^2] \frac{dW}{d\phi} \right\} \\
 N_\phi &= \frac{D}{R^3} \left\{ \frac{d^4 W}{d\phi^4} + [1 - 2(1-\nu)m^2] \frac{d^2 W}{d\phi^2} \right\} \\
 \frac{dS}{dx} &= -\frac{D}{R^4} \left\{ \frac{d^5 W}{d\phi^5} + [2 - 2(1-\nu)m^2] \frac{d^3 W}{d\phi^3} \right\} \\
 N_x &= -\frac{D}{R^3 m^2} \left\{ \frac{d^6 W}{d\phi^6} + [2 - 2(1-\nu)m^2] \frac{d^4 W}{d\phi^4} \right\}. \tag{9}
 \end{aligned}$$

Now $W = Ae^{p\phi}$ where A and p have eight complex values. Before we can tackle the design of the shell roof we have to be able to extract W and its derivatives in terms of real constants and quantities. A simple method of doing this will now be outlined.

TO OBTAIN THE DERIVATIVES OF A SOLUTION TO A LINEAR DIFFERENTIAL EQUATION

Two terms of the solution will be taken in the form:

$$W = A_1 e^{p_1 \phi} + A_2 e^{p_2 \phi}$$

where

$$p_1 = \beta + \alpha i \quad p_2 = \beta - \alpha i.$$

Then

$$d^n W/d\phi^n = A_1 p_1^n e^{p_1 \phi} + A_2 p_2^n e^{p_2 \phi}.$$

It is always possible to express β as $k \cos \theta$ and α as $k \sin \theta$. Now

$$e^{i\alpha\phi} = \cos \alpha\phi + i \sin \alpha\phi$$

and

$$(k \cos \theta + ik \sin \theta)^n = k^n (\cos n\theta + i \sin n\theta)$$

from DeMoivre's theorem.

$$\begin{aligned} \therefore d^n W/d\phi^n &= A_1 (\beta + \alpha i)^n e^{\beta\phi} e^{\alpha i\phi} + A_2 (\beta - \alpha i)^n e^{\beta\phi} e^{-\alpha i\phi} \\ &= A_1 k^n (\cos n\theta + i \sin n\theta) e^{\beta\phi} (\cos \alpha\phi + i \sin \alpha\phi) \\ &\quad + A_2 k^n (\cos n\theta - i \sin n\theta) e^{\beta\phi} (\cos \alpha\phi - i \sin \alpha\phi) \\ &= k^n e^{\beta\phi} \{ [(A_1 + A_2) \cos n\theta + (A_1 - A_2) i \sin n\theta] \cos \alpha\phi \\ &\quad + [-(A_1 + A_2) \sin n\theta + (A_1 - A_2) i \cos n\theta] \sin \alpha\phi \}. \end{aligned}$$

Putting $A_1 + A_2 = C1$ and $(A_1 - A_2)i = C2$

$$d^n W/d\phi^n = k^n e^{\beta\phi} \{ (C1 \cos n\theta + C2 \sin n\theta) \cos \alpha\phi + (-C1 \sin n\theta + C2 \cos n\theta) \sin \alpha\phi \}.$$

In matrix form this is conveniently put as

$$k^n [\cos n\theta \quad \sin n\theta] e^{\beta\phi} \begin{bmatrix} \cos \alpha\phi & \sin \alpha\phi \\ -\sin \alpha\phi & \cos \alpha\phi \end{bmatrix} \begin{bmatrix} C1 \\ C2 \end{bmatrix} \quad \text{or } A.B.C.$$

where A depends on the order of the derivative, B the angular position in the shell, and C is the vector containing the constants of integration.

DEVELOPING THE PROGRAM

The roots of the simplified Flügge equation form two sets

$$(1) \quad p^2 = -\frac{1}{2} + m^2 + mK \pm mKi = R1 \pm mKi$$

$$(2) \quad p^2 = -\frac{1}{2} + m^2 - mK \pm mKi = -R2 \pm mKi.$$

We shall take first the first set with the positive imaginary part.

$$k_1^2 (\cos 2\theta_1 + i \sin 2\theta_1) = R_1 + mKi$$

$$\tan 2\theta_1 = mK/R_1 \quad \text{or} \quad \theta_1 = \frac{1}{2} \arctan(mK/R1)$$

$$\begin{aligned} k_1^4 \cos^2 2\theta_1 &= R_1^2 \\ \frac{k_1^4 \sin^2 2\theta_1}{k_1^4} &= \frac{m^2 K^2}{R_1^2 + m^2 K^2} \end{aligned}$$

$$\therefore k_1 = \sqrt[4]{(R_1^2 + m^2 K^2)}.$$

Taking now the second set with the positive imaginary part

$$\tan 2\theta_2 = -mK/R_2 \quad \therefore \theta_2 = \frac{1}{2}(\pi - \arctan mK/R_2)$$

$$k_2 = \sqrt[4]{(R_2^2 + m^2 K^2)}.$$

Then

$$\begin{aligned} \beta_1 &= k_1 \cos \theta_1 & \alpha_1 &= k_1 \sin \theta_1 \\ \beta_2 &= k_2 \cos \theta_2 & \alpha_2 &= k_2 \sin \theta_2. \end{aligned}$$

The matrices for the derivations can now be set out as follows:

A will be an 8 × 8 matrix with rows corresponding to the *n* values required (−1 to 6) and columns having the values

$$k_1^n \cos n\theta_1 \quad k_1^n \sin n\theta_1 \quad (-k_1)^n \cos n\theta_1 \quad (-k_1)^n \sin n\theta_1 \quad k_2^n \cos n\theta_2 \quad \dots$$

B will also be an 8 × 8 matrix as follows

<i>B</i> ₁	O	O	O
O	<i>B</i> ₂	O	O
O	O	<i>B</i> ₃	O
O	O	O	<i>B</i> ₄

$$B_1 = e^{\beta_1 \phi} \begin{bmatrix} \cos \alpha_1 \phi & \sin \alpha_1 \phi \\ -\sin \alpha_1 \phi & \cos \alpha_1 \phi \end{bmatrix}$$

$$B_2 = e^{-\beta_1 \phi} \begin{bmatrix} \cos \alpha_1 \phi & -\sin \alpha_1 \phi \\ \sin \alpha_1 \phi & \cos \alpha_1 \phi \end{bmatrix}, \text{ etc.}$$

C will be a 1 × 8 column matrix containing the eight constants of integration *C*₁ ... *C*₈.

A new 8 × 8 matrix *D* is now produced, the row number corresponding to the order of the highest derivative in the expression for the shell displacement or stress. This is done by employing equations (9).

For *j* having the values 1–8

$$D_{-1j} = A_{-1j} \quad v$$

$$D_{0j} = A_{0j} \quad w$$

$$D_{1j} = \frac{1}{R}(A_{1j} + A_{-1j}) \quad a$$

$$D_{2j} = -\frac{D}{R^2}(A_{2j} + A_{0j}) \quad M_\phi$$

$$D_{3j} = -\frac{D}{R^3}(A_{3j} + K_1 A_{1j}) \quad V_\phi$$

$$D_{4j} = \frac{D}{R^3}(A_{4j} + K_1 A_{2j}) \quad N_\phi$$

$$D_{5j} = -\frac{D}{R^4}(A_{5j} + K_2 A_{3j}) \quad dS/dx$$

$$D_{6j} = -\frac{D}{R^3 m^2}(A_{6j} + K_2 A_{4j}) \quad Nx$$

where

$$K_1 = 1 - 2(1 - \nu)m^2$$

and

$$K_2 = 2 - 2(1 - \nu)m^2.$$

STRESSES DUE TO POST-TENSIONING

The handling of the gravity loading of the shell is too well known to require repetition [2, 5]. However the usual method of replacing the post tension by the Fourier series

$$\frac{4P}{\pi} \sum_{N=1,3,5,\dots}^{\infty} \frac{1}{N} \sin \frac{N\pi}{2} \cos \frac{N\pi x}{L} \tag{10}$$

leads to serious difficulties.

This is due to the shear at the edge of the shell being proportional to the rate of change of the force in the edge beam, or the differential of (10) which can be seen to oscillate with increasing number of terms near the centre of the shell and diverge near the traverses (Fig. 3a).

A more satisfactory series is obtained by assuming that the post tension is fed into the edge beam by shearing forces decreasing linearly from the traverse to the quarter points. This produces the parabolic distribution of post tension shown in Fig. 3(b).

The Fourier series for this is

$$\sum P_N \cos \frac{N\pi x}{L} = \sum_{N=1,3,5,\dots}^{\infty} \frac{128P}{(N\pi)^3} \left(\sin \frac{N\pi}{2} - \sin \frac{N\pi}{4} \right) \cos \frac{N\pi x}{L} \tag{11}$$

Four terms of this series summed up on a desk computer showed almost perfect agreement with the curve chosen and can be differentiated without much loss of accuracy.

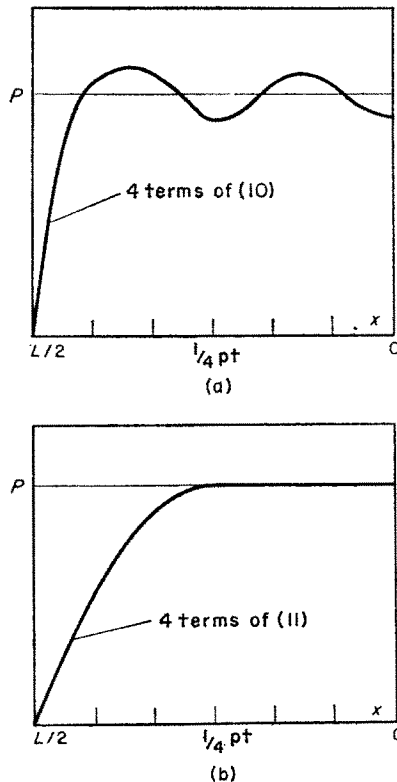


Fig. 3. Fourier series for post tension.

ANALYSIS OF SHELL WITH TUBULAR EDGE BEAM

The theory was tested on the model shell with a tubular edge beam described in the next section. In this special case the stresses and deformations are produced only by the post tensioning, there being no gravity loading on the shell. The boundary conditions for the model shell can be expressed fairly simply as follows:

The B matrix is calculated for the right hand edge. This is multiplied by the D matrix to give matrix E (8 × 8) which relates to the shell displacements, moments and forces for the right hand edge when multiplied by the C vector. The numerical values for the boundary conditions are put in the G vector.

The four boundary conditions for the right hand edge can then be put into the first four rows of matrix F (8 × 8) and vector G (8 × 1) as follows:

(1) The rotations of the shell edge and the edge beam are equal. Reference to Fig. 4(a) shows that

$$\begin{aligned} \frac{dT}{dx} &= (M_\phi + bN_\phi)\cos \frac{N\pi x}{L} \\ \frac{da}{dx} &= -\frac{T}{GJ} \\ a &= \frac{1}{GJ} \iint (M_\phi + bN_\phi)\cos \frac{N\pi x}{L} dx dx \\ &= \left(\frac{L}{N\pi}\right)^2 \frac{1}{GJ} (M_\phi + bN_\phi) \text{ at } x = 0. \end{aligned}$$

Then for j having values from 1 to 8

$$\begin{aligned} F_{1j} &= E_{1j} - \left(\frac{L}{N\pi}\right)^2 \frac{1}{GJ} (E_{2j} + bE_{4j}) \\ G_1 &= 0. \end{aligned}$$

(2) The radial displacements w of the shell and the edge beam are equal. Reference to Fig. 3(d) shows that

$$\begin{aligned} dt &= S dx \\ t &= \iint \frac{dS}{dx} dx dx \text{ at } x = 0 \\ &= -\left(\frac{L}{N\pi}\right)^2 \frac{dS}{dx}. \end{aligned}$$

For the edge beam

$$\begin{aligned} -EI \frac{d^4w}{dx^4} &= V_\phi \cos \frac{N\pi x}{L} \\ M &= -EI \frac{d^2w}{dx^2} = \left\{ -\left(\frac{L}{N\pi}\right)^2 V_\phi + tb \right\} \cos \frac{N\pi x}{L} \\ \therefore w &= -\frac{1}{EI} \left(\frac{L}{N\pi}\right)^2 \left\{ \left(\frac{L}{N\pi}\right)^2 V_\phi + b\left(\frac{L}{N\pi}\right)^2 \frac{dS}{dx} \right\} \\ F_{2j} &= E_{0j} + \frac{1}{EI} \left(\frac{L}{N\pi}\right)^4 \{E_{3j} + bE_{5j}\} \\ G_2 &= 0. \end{aligned}$$

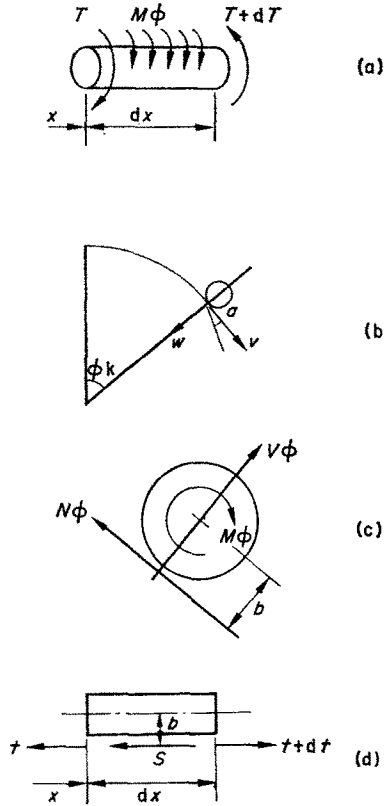


Fig. 4. Element of tubular edge beam.

(3) The tangential displacements v of the shell and the edge beam are equal.

$$EI \frac{d^4 v}{dx^4} = -N_\phi \cos \frac{N\pi x}{L}$$

$$\therefore v = -\frac{1}{EI} \left(\frac{L}{N\pi}\right)^4 N_\phi \text{ at } x = 0$$

$$F_{3j} = E_{-1j} + \frac{1}{EI} \left(\frac{L}{N\pi}\right)^4 E_{4j}$$

$$G_3 = 0.$$

(4) The longitudinal strains of the shell and the edge beam are equal. The strain in the edge beam is

$$\frac{t - P_N}{EA}$$

due to the longitudinal force. The strain in the edge beam at the springing due to bending is

$$-b \frac{d^2 w}{dx^2} = b \left(\frac{N\pi}{L}\right)^2 w \text{ at } x = 0.$$

The strain in the shell at the springing is

$$\frac{1}{EI}(N_x - \nu N_\phi)$$

$$F_{4j} = \frac{1}{Eh}(E_{6j} - \nu E_{4j}) + \frac{1}{EA}\left(\frac{L}{N\pi}\right)^2 E_{5j} - b\left(\frac{N\pi}{L}\right)^2 E_{0j}$$

$$G_4 = -P_N/EA.$$

The *B* matrix is then recalculated for the left hand edge. A new *E* matrix is produced by multiplying *B* by *D*. The second half of the *F* and *G* matrices can then be filled in a similar manner to the first, making allowance for some sign differences.

The eight simultaneous equations represented by *FC = G* are solved to find the integration constants *C*. The shell stresses and displacements can then be calculated from *D.B.C.*, the change in angular position modifying only *B*.

CORRECTION AT CORNERS OF PRESTRESSED SHELL

The boundary conditions assumed in the foregoing analysis imply that *N_x* is zero at the traverses. This means that compatibility of strain cannot apply at the ends of the edge beam where the strain is the greatest.

It is evident that the traverses can transmit some of the post tension and this is allowed for in the following correction which is added to the previous solution.

It will be supposed that the post tension is returned to the corners of the shell by applying shear forces *S1* to the edge beam and *S2* to the shell edge, both varying linearly from the quarter points to the traverse. These will produce the parabolic variation of longitudinal stress shown in Fig. 5 and will be apportioned to retain compatibility of strain.

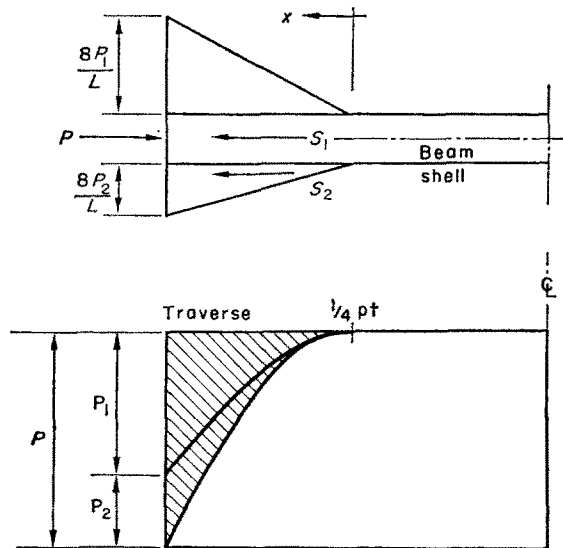


Fig. 5. Correction at corners of shell.

The characteristic equation of the shell will be taken in its simplest form:

$$\frac{\partial^8 u}{\partial \phi^8} + 4K^4 R^4 \frac{\partial^4 u}{\partial x^4} = 0. \tag{12}$$

The longitudinal strain $\partial u/\partial x$ will vary with x^2

$$\therefore \frac{\partial^4 u}{\partial x^4} = 0.$$

Equation (12) then reduces to $\partial^8 u/\partial \phi^8 = 0$. Then

$$\frac{\partial u}{\partial x} = (C_1 \phi^7 + C_2 \phi^6 + C_3 \phi^5 \dots C_8)x^2.$$

Assuming symmetry about the ζ , $f(\phi) = f(-\phi)$ and C_1, C_3, C_5, C_7 are zero. If the traverse is fairly flexible in the x direction the forces produced by the end correction will die away rapidly from the edge. It is also clear that only compatibility of strain with the edge beam is of importance. The solution to (12) will then be taken as

$$\partial u/\partial x = C_2 \phi^6 x^2. \tag{13}$$

If ϵ is the longitudinal strain at the corners of the shell

$$N_x = Eh\phi^6 \epsilon 16x^2/L^2 = Eh\epsilon \phi^6 \text{ at } x = L/4.$$

Then

$$P_2 = \int_0^{\phi_K} N_x R d\phi = EhR\epsilon \phi_K^7 / 7$$

$$P_1 = EA\epsilon \text{ at } x = L/4.$$

Then

$$P = E\epsilon(A + Rh\phi_K^7/7) \tag{14}$$

from which ϵ, P_1 and P_2 can be calculated.

EXPERIMENT

A small steel model shell roof was constructed as shown in Fig. 6. Tubular edge beams were soldered on to the edges of the shell. A steel rod was passed through one of the edge beams and stressed by means of nuts screwed on the ends. Buckling was avoided by fixing the tendon at the centre with set screws. The strains along the edge beam were measured with eight pairs of Huggenberger tensometers.

The magnitude of the post tension was obtained from the strain of those portions of the edge beam that extended beyond the shell.

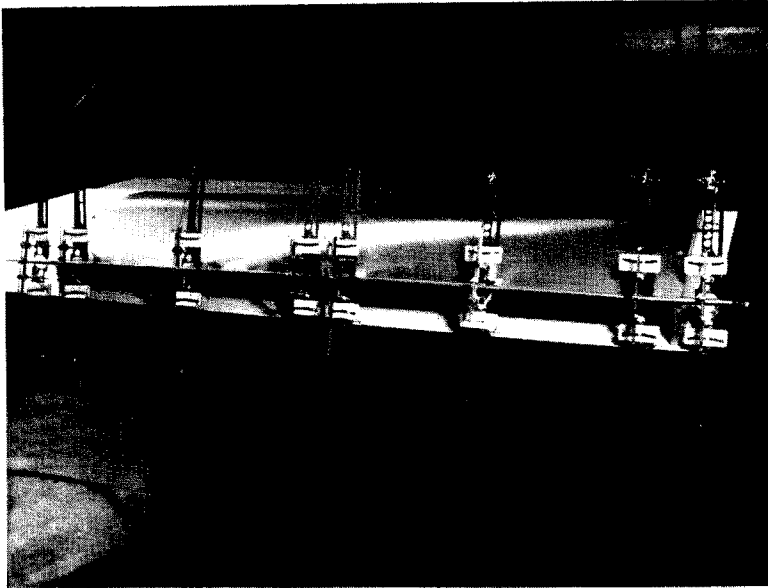


Fig. 6. Model steel shell with tensometers $L = 36$ in., $R = 12$ in., $h = 0.031$ in. Half angle $\phi_K = 40^\circ$, $A = 0.02112$ in², $b = 0.1715$ in.

COMPARISON OF THEORY WITH EXPERIMENT

The strains in the edge beam of the model shell were calculated using the simplified Flügge method described and summing up the Fourier series (11) using values of $N = 1, 3, 5, 7$. The results were in excellent agreement with the measured values in the centre half of the shell. The addition of the corner correction took the agreement to the outer portion of the edge beam. This is shown in Fig. 7.

A further check on the method was made by analysing a shell with a rectangular edge beam and comparing the results with a finite element program[6]. Good agreement was once more obtained as is seen in Fig. 8. The handling of the corner correction in this case is shown in the appendix.

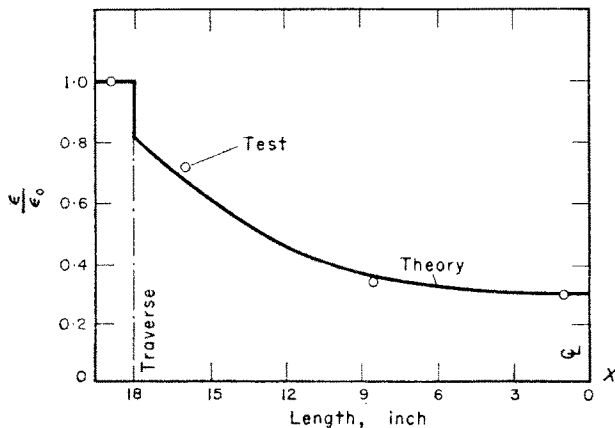


Fig. 7. Comparison of theory with model.

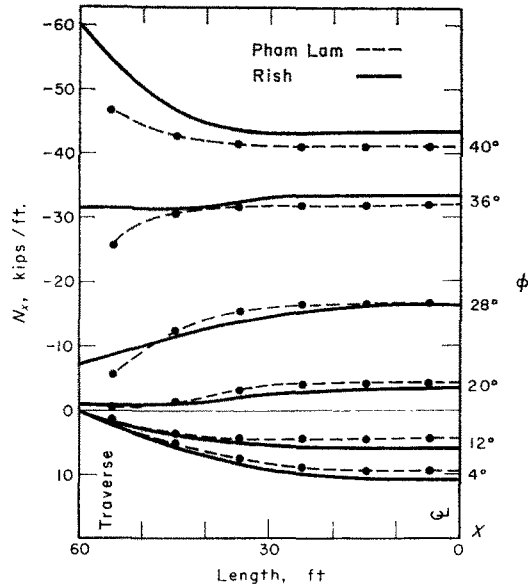


Fig. 8. Comparison of theory with finite element analysis.

REFERENCES

1. W. Flügge, *Stresses in Shells*. Springer, Berlin (1966).
2. R. Dombrowski, Analysis of prestressed cylindrical shell roofs, *J. Struct. Div. Am. Soc. civ. Engrs.* **89**, 91-116 (1963).
3. J. E. Gibson, *The Design of Cylindrical Shell Roofs*. Spon (1961).
4. N. J. Hoff, The accuracy of Donnell's equations, *J. appl. Mech.* **77**, 329-334 (1955).
5. G. J. Ramaswamy, *Design and Construction of Concrete Shell Roofs*. McGraw-Hill, New York (1968).
6. Pham Lam, M.Eng. Thesis, University of Tasmania (1972).

Абстракт — Для перекрытий в форме цилиндрической оболочки определяется новое характеристическое уравнение, вместе с методом получения решения и его производных. Применяется предварительное натяжение бортовой балки посредством сдвиговых усилий, которые изменяются линейно от максимума в месте поперечной балки к нулю в четверти пролета. Для этого случая ряд Фурье сходится быстро. Далее приводится краевая корректировка с целью обратной передачи предварительного натяжения к краю балки и получения совместности деформации на краю оболочки. Сравняется метод с экспериментальными результатами на модели оболочки и с результатами программы конечного элемента.

APPENDIX

Analysis of shell with post tensioned rectangular edge beams (Fig. 9.)

$$P = 500 \text{ kips}$$

$$L = 120 \text{ ft} \quad A = 2 \text{ sq ft}$$

$$R = 30 \text{ ft}$$

$$h = 0.25 \text{ ft}$$

$$\phi_k = 40^\circ = 0.698 \text{ rad.}$$

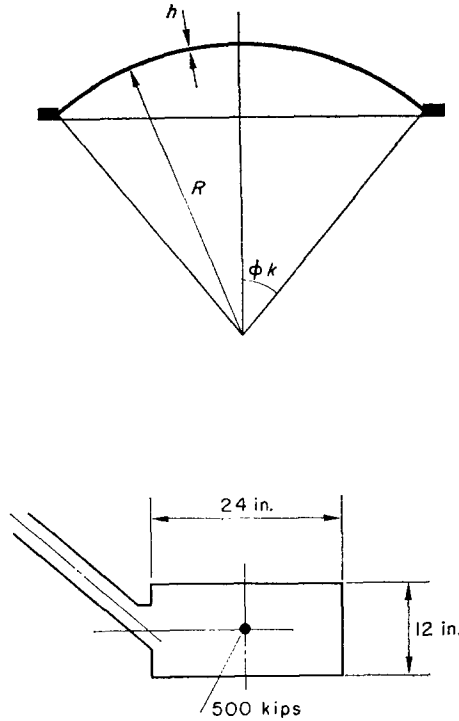


Fig. 9. Rectangular edge beam.

$$P = E\varepsilon(A + Rh\phi_k^7/7) = EA(2 + 0.087)$$

$$= E\varepsilon \times 2.087 = 500 \text{ kips.}$$

At corner

$$N_x = hE\varepsilon = 0.25 \times 500/2.087 = 60 \text{ kips/ft.}$$

This edge correction will diminish with ϕ to the 6th power of ϕ/ϕ_k as follows

ϕ/ϕ_k	1	0.9	0.8	0.7	0.6	0.5	0.4
Factor	1	0.531	0.262	0.118	0.047	0.016	0.004

It will also diminish parabolically back to zero at the 1/4 points of the shell. The N_x values obtained from (8) are as follows:

N	P_N kips	N_x $\phi = 40$	N_x $\phi = 36^\circ$
1	604.56	-52.292	-39.773
3	-130.50	10.931	7.572
5	28.19	-2.243	-13.321
7	-1.76	0.141	0.069

	Sum Fourier series	Edge correc- tion	Total $\phi = 36^\circ$	Sum Fourier series	Edge correc- tion	Total $\phi = 40^\circ$
Traverse	0	31.860	31.860	0	60.000	60.00
	17.002	14.160	31.162	23.566	26.666	50.232
	28.090	3.540	31.630	38.127	6.666	44.793
1/4 pt.	32.487	0	32.487	43.020	0	43.020
	33.351	0	33.351	43.466	0	43.466
	33.427	0	33.427	43.398	0	43.398
Ⓢ	33.464	0	33.464	43.463	0	43.463